Measurement of the Electroweak Correction to $A_\perp$ in Polarized Electron-Nucleon Scattering

A thesis submitted in partial fulfillment of the requirement
for the degree of Bachelor of Science with Honors in
Physics from the College of William and Mary in Virginia,

by

Patrick D. Ryan

Accepted for ______________________________
(Honors, High Honors or Highest Honors)

____
Advisor: Dr. Keith Griffioen

____
Dr. Todd Averett

____
Dr. Morton Eckhause

____
Dr. Gina Hoatson

____
Dr. George Rublein

____
Dr. Shiwei Zhang

Williamsburg, Virginia
May 2000

Abstract

Experiment E155x at the Stanford Linear Accelerator Center measured deep inelastic scattering of longitudinally polarized electrons from transversely polarized proton and deuteron targets to determine the A_2 virtual photon asymmetry and the g_2 structure function. The measured asymmetries in the experiment contain a sizable electroweak contribution. This electroweak asymmetry can be extracted directly from the data and compared to standard model calculations. The experimental value for the electroweak asymmetry is $-7.19 \times 10^{-5} \pm 1.37 \times 10^{-5}$. This result agrees with the calculated theoretical prediction of -7.88×10^{-5} within statistical errors.

Acknowledgements

I would first like to thank my advisor Keith Griffioen, who has helped me in so many ways. He gave me the opportunity to conduct research at SLAC, patiently answered my all my questions, and gave excellent guidance throughout my research. I would also like to thank the people at SLAC and in the E155x collaborations for all their help, especially Lee Sorrell and Greg Mitchell. Finally I would like to acknowledge Ian Swason and Brian Tighe who kept me company during the 10 hour-days spent in computer lab while writing this thesis.

Contents

1 Introduction

1.1 Overview of Spin Structure Experiments

In 1989, experiments at CERN [1] reported results that contradicted the Quark Parton Model (QPM) of nucleon spin, which predicts that the valence quarks are the sole contributors to the spins of protons and neutrons. Since this "spin crisis," both theoretical and experimental studies have been conducted to understand the contributions of gluon spin and quark-gluon angular momentum to nucleon spin. Experiments at CERN [2], SLAC [3]-[6], and DESY [7],[8] have measured these contributions with increasing precision, and E155x is a continuation of this effort [9]. The purpose of E155x is to measure the transverse asymmetries using deep inelastic scattering of longitudinally polarized electrons from transversely polarized targets to determine the virtual photon-nucleon asymmetries A_2^p and A_2^d and the structure functions g_2^p, g_2^d, and g_2^n [9]. A list of the previous spin structure experiments and the quantities measured is given in Table 1. The asymmetries were measured using parallel ($\|$) and perpendicular ($\perp$) target polarizations for protons (p), neutrons (n), and deuterons (d) [1]-[12].

1.2 Kinematics of Deep Inelastic Scattering

Polarized deep inelastic scattering (DIS) is used to study the spin structure of nucleons. In inclusive DIS, only electrons which scatter from the quarks inside the nucleon are detected. The kinematics are shown in Figure 1. In this figure q^μ is the 4-momentum transferred to the nucleon by the virtual photon, $Q^2 \equiv -q^\mu q_\mu$ is the 4-momentum transfer squared, E is the energy of the incident electron, E' is the energy of the scattered electron, and ν is the energy transfer $E - E'$.

It can be shown that $Q^2 \equiv -q^\mu q_\mu = 4EE' \sin^2 \frac{\theta}{2}$ where θ is the laboratory scattering angle. The Bjorken scaling variable x, which gives the fraction of the nucleon

Table 1: The history of spin structure experiments.

Year	Experiment	Data	Target
1978	E80	$A_\parallel^p$	Butanol
1983	E130	$A_\parallel^p$	Butanol
1988	EMC	$A_\parallel^p$	NH_3
1991	SMC	$A_\parallel^d$	Butanol
1992	E142	$A_\parallel^n$,$A_\perp^n$	^{3}He
1993	SMC	$A_\parallel^p$,$A_\perp^p$	Butanol
1994	E143	$A_\parallel^p$,$A_\perp^p$,$A_\parallel^n$,$A_\perp^n$	$^{15}NH_3$,$^{15}ND_3$
1994	SMC	$A_\parallel^d$	Butanol
1995	SMC	$A_\parallel^d$	Butanol
1995	SMC	$A_\parallel^d$	Butanol
1995	HERMES	$A_\parallel^n$	^{3}He
1995	E154	$A_\parallel^n$,$A_\perp^n$	^{3}He
1996	SMC	$A_\parallel^p$	NH_3
1996	HERMES	$A_\parallel^p$	H_1,H_2,^{3}He,^{14}N
1997	E155	$A_\parallel^p$,$A_\perp^p$,$A_\parallel^n$,$A_\perp^n$	NH_3
1999	E155x	$A_\parallel^n$,$A_\perp^n$	NH_3,LiD

momentum carried by the struck quark, is

$$x \equiv \frac{Q^2}{2M\nu} = \frac{Q^2}{2M(E - E')}. \quad (1)$$

By measuring only E' and θ, both x and Q^2 can be determined, which together fully describe electron-nucleon scattering.

The kinematics range of E155x is shown in Figure 2. It can be seen that each spectrometer covers a different band in the x vs. Q^2 plane.

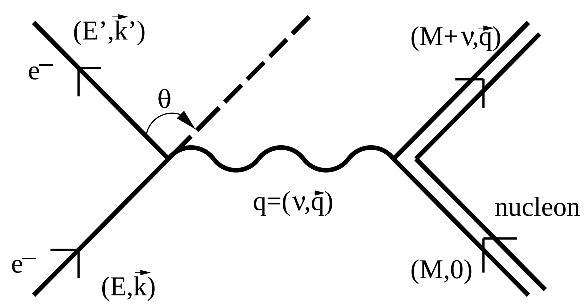

Figure 1: Kinematics of Deep Inelastic Scattering

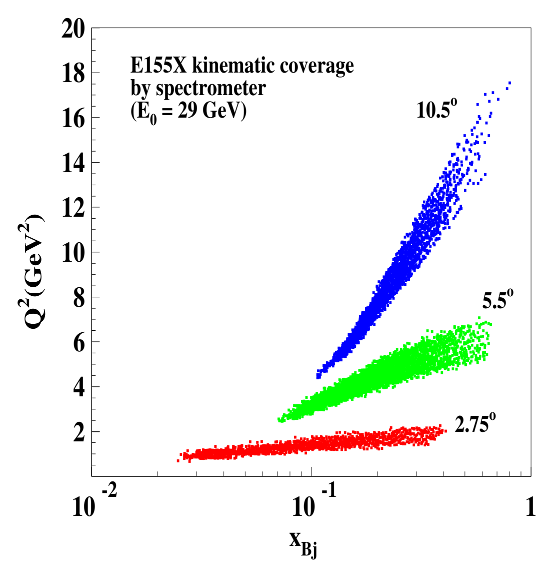

Figure 2: Kinematics of Deep Inelastic Scattering for scattering at $\theta = 2.75°$, $5.5°$, and $10.5°$.

1.3 Polarized Deep Inelastic Scattering

For an unpolarized target, the cross section can be related to the unpolarized structure functions F_1 and F_2 by

$$\frac{d\sigma}{d\Omega dE'} = \frac{4\alpha^2 E'^2 \cos^2\left(\frac{\theta}{2}\right)}{Q^4}\left[\frac{F_2(x,Q^2)}{\nu} + \frac{2F_1(x,Q^2)}{M}\tan^2\left(\frac{\theta}{2}\right)\right] \tag{2}$$

where M is the nucleon mass and θ is the laboratory scattering angle. The structure function F_1, in the limit of high Q^2, is

$$F_1(x,Q^2) = \frac{1}{2}\sum_i e_i^2[q_i^\uparrow(x,Q^2) + q_i^\downarrow(x,Q^2)] \tag{3}$$

where $q_i^{\uparrow}(x,Q^2)$ and $q_i^{\downarrow}(x,Q^2)$ are the probability distributions for the ith quark flavor to be aligned and anti-aligned, respectively, with the nucleon spin. The index i in the summation is over the kinematically allowed quark flavors, and e_i is the corresponding quark charge [14]. In the scaling limit of high Q^2,

$$F_2 = 2xF_1. \tag{4}$$

For a polarized beam and target, the polarized structure function g_1 is given by

$$g_1(x,Q^2) = \frac{1}{2}\sum_i e_i^2[q_i^{\uparrow}(x,Q^2) - q_i^{\downarrow}(x,Q^2)] \equiv \sum_i e_i^2 \Delta q_i(x,Q^2). \tag{5}$$

Note that g_1 measures the difference in the quark helicities instead of the sum, as in F_1. In the scaling limit the g_2 structure function is a convolution of g_1 and is given by the Wandzura-Wilczek form [16]

$$g_2^{WW}(x,Q^2) = -g_1(x,Q^2) + \int_x^1 \frac{g_1(y,Q^2)}{y}dy. \tag{6}$$

The g_1 and g_2 structure functions are determined from the cross section asymmetries

$$A_{\|} = \frac{\sigma^{\downarrow\uparrow} - \sigma^{\uparrow\uparrow}}{\sigma^{\downarrow\uparrow} + \sigma^{\uparrow\uparrow}} = f_k\left(g_1(x,Q^2)[E + E'\cos\theta] - \frac{Q^2}{\nu}g_2(x,Q^2)\right) \tag{7}$$

$$A_{\perp} = \frac{\sigma^{\downarrow\leftarrow} - \sigma^{\uparrow\leftarrow}}{\sigma^{\downarrow\leftarrow} + \sigma^{\uparrow\leftarrow}} = f_k E'\sin\theta\left(g_1(x,Q^2) + \frac{2E}{\nu}g_2(x,Q^2)\right), \tag{8}$$

where f_k, which includes the unpolarized structure function F_1 and the ratio R of the transverse and longitudinal virtual photon cross section, is

$$f_k = \frac{1-\epsilon}{\nu F_1(x_1,Q^2)[1+\epsilon R(x,Q^2)]}, \tag{9}$$

with

$$\epsilon = \left[1 + 2\left(1 + \frac{\nu^2}{Q^2}\right)\tan^2(\theta/2)\right]^{-1}. \tag{10}$$

The first arrows in the cross section asymmetry represent the beam helicities and the second arrows represent the target spin direction. The asymmetries were measured with both positive and negative target polarizations to minimize systematic effects. For the small values of θ used in the SLAC experiments, $A_{\|}$ is mainly sensitive to g_1 and $A_\perp$ to g_2. E155x was concerned with measuring g_2 [14]. A schematic representation of the beam and target polarizations is given in Figure 3.

The above asymmetry formulas can be solved for g_1 and g_2 to obtain

$$g_1(x,Q^2) = \frac{F_1(x,Q^2)}{d'}[A_\parallel + \tan(\theta/2)A_\perp] \qquad \text{and} \tag{11}$$

$$g_2(x,Q^2) = \frac{yF_1(x,Q^2)}{2d'}\left[\frac{E+E'\cos(\theta)}{E'\sin(\theta)}A_\perp - A_\parallel\right] \tag{12}$$

where $y = (E-E')/E$, $d' = [(1-\epsilon)(2-y)]/[y(1+\epsilon R(x,Q^2))]$, and $R(x,Q^2) = \frac{\sigma_L}{\sigma_R}$ is the ratio of longitudinal and transverse virtual photon cross sections.

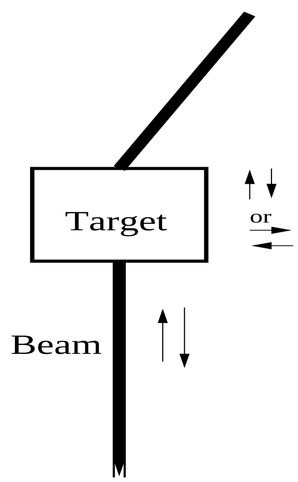

Figure 3: Polarizations of Beam and Target

2 The Experiment

The SLAC Linear Accelerator is a two mile long electron/positron accelerator. The target was located in End Station A. E155x ran for a two month period in the spring of 1999.

2.1 The Electron Source

Polarized electrons were produced by laser photo-emission from a strained GaAs source. Straining was accomplished by growing a 100nm thick epitaxial layer of GaAs on a $GaAs_{(1-x)}P_x$ substrate. The smaller lattice spacing in the substrate caused the strain on the GaAs, which resulted in the removal of the spin state degeneracy.

The photo-emission of electrons was caused by illuminating the surface of the GaAs with a laser and the helicity of the electron polarization was determined by the sign of the circular polarization of the laser light. The pattern of polarization was chosen using a 32-bit random number generator to minimize instrumental asymmetries [4].

2.2 The Beam

The beam consisted of 120 spills per second of 400 ns length, with an average current of 25 nA. The electrons traveling down the accelerator were deflected 24.5° in the A-line beam transport and directed onto the polarized target in End Station A. The electron has an anomalous magnetic moment, and therefore its spin precesses by an angle larger than that of the 24.5° bend in the beam. This precession is described by

$$\Delta\phi = \pi \left(\frac{24.5^\circ}{180^\circ}\right) \left(\frac{g-2}{2}\right) \left(\frac{E}{m}\right) = \left(\frac{E}{3.237}\right) \pi \tag{13}$$

where g is the gyromagnetic ratio, E is the energy (in GeV), m is the mass of the electron, and $\Delta\phi$ is the angle between the electron's spin and its momentum at the target. When $\Delta\phi$ is an integral multiple of π, the electron is polarized longitudinally to the beam momentum. Electrons with odd integer values of $\frac{\Delta\phi}{\pi}$ have opposite spins to those with even integers. E155x ran at beam energies of 29.1 and 32.3 GeV, which have $\Delta\phi$ values of 9π and 10π, respectively. Therefore, at these different beam energies, electrons with the same original spin directions have opposite spin polarizations at the target [4].

The beam polarization was measured using $e^- \to e^-$ scattering from an iron Møller target. The beam polarization was stable over all runs and for the main analysis an average polarization of 83% was used.

2.3 The Target

E155x used two different polarized targets: NH_3 for proton scattering, and LiD for deuteron scattering. A schematic diagram of the target is shown in Figure 4. A liquid helium refrigerator was used to cool the target down to 1 K and a superconducting magnet generated a field of 5 T. The different targets were placed along an insert which was raised and lowered along the central axis of the target in order to select the different target types. The targets were ^{6}LiD, $^{15}NH_3$, empty, and carbon or beryllium. The average polarization for the ^{6}LiD target was 22%, and for the $^{15}NH_3$ target the average polarization was 75%.

Dynamic nuclear polarization (DNP) was used to polarize the protons and deuterons [4]. This process entailed transferring atomic electron polarization in the material, caused by the magnetic field, to the nucleons through a hyperfine transition by irradiating the target with microwaves.

The polarization decreased as the target became damaged by radiation. When the target polarization fell below a certain pre-determined value, the next target on the insert was put into the beam. After both targets had been radiation damaged, they were annealed by warming them to approximately 80 K [4] to repair this damage.

2.4 Spectrometers

The scattered electrons were detected in three spectrometers located at angles of 2.75°, 5.5°, and 10.5° with respect to the beam line, as shown in Figure 5. Figure 6 shows a side view of the spectrometers.

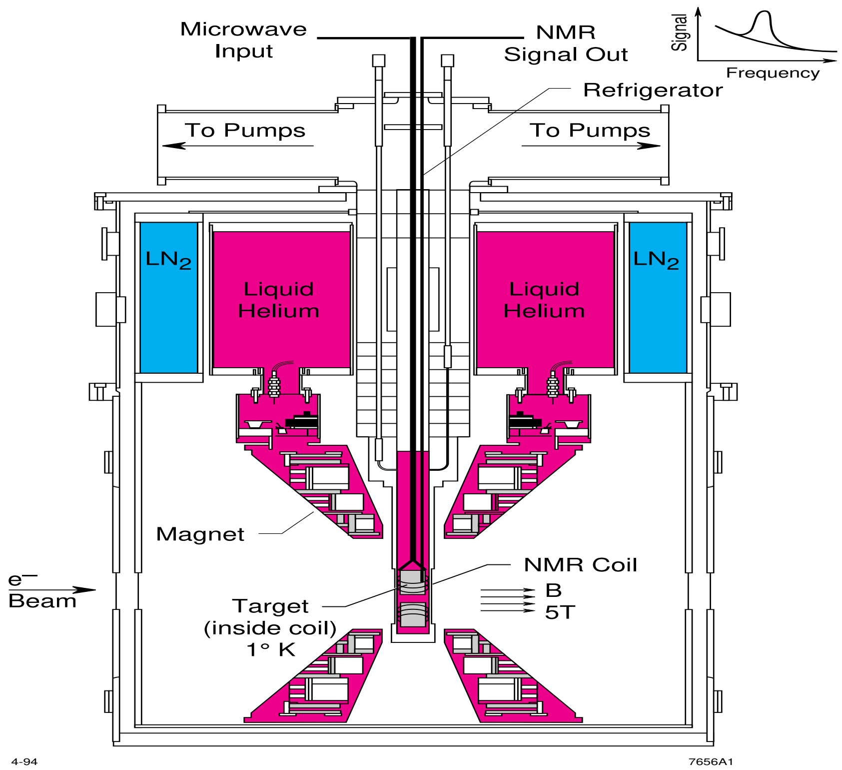

Figure 4: Schematic diagram of the polarized target.

2.4.1 Magnets

The 2.75° and 5.5° spectrometers included two dipole magnets and the 10.5° spectrometer included one. These magnets bent particles in opposite directions in the vertical plane. The purpose of these was to perform a momentum selection on the scattered particles and to shield the detectors from a considerable photon background by requiring the particles to scatter at least twice in order to reach the spectrometers. In addition, two quadrupole magnets were included in the 10.5° and one in the 2.75° spectrometer. These magnets served to disperse the scattered particles evenly across the detectors and increase the solid angle detected.

2.4.2 Cherenkov Tanks

Two Cherenkov tanks were located in the 2.75° and 5.5° spectrometers and one in the 10.5° spectrometer, and were used to distinguish electrons from pions and other heavier particles. These tanks were filled with gaseous N_2 and CH_4. The threshold for Cherenkov light was set to select electrons against heavier particles such as pions.

2.4.3 Scintillator Hodoscopes

Two scintillator hodoscope packages were located in the 2.75°, 5.5°, and 10.5° spectrometers (only one is shown for the 10.5° spectrometer in Figure 5 since this figure was generated for E155). These detectors consisted of approximately three-foot long, one-inch wide, and one-quarter-inch thick fingers of scintillating plastic. The plastic was wrapped in aluminum foil and electrical tape to reduce light loss and connected to a photomultiplier tube at one end which recorded a light signal. The fingers were layered and aligned in horizontal and vertical arrays. They were used to measure the position, and thus the momentum, of the scattered electrons.

2.4.4 Electromagnetic Shower Counters

The shower counters consisted of lead glass total absorber (TA) blocks. The 2.75° and 5.5° spectrometers contained a 20 by 10 array of blocks that were $2\frac{1}{2} \times 2\frac{1}{2}$ inches. The total absorber section in the 10.5° spectrometer consisted of a five by six array of blocks approximately six inches square. Photomultiplier tubes were connected to the back of the total absorber blocks. A pre-radiator section was added to the 10° spectrometer and consisted of a vertical stack of ten horizontal bars of approximately one meter in length and $2\frac{1}{2}$ inches wide. Photomultiplier tubes were attached to each end of the blocks.

Electrons and positrons produce Cherenkov light with an intensity proportional to their energy as they shower through the lead glass. The shower is created as an electron or positron radiates a photon in the large Coulomb field of the lead nuclei, which in turn pair produces to form another electron and positron. This happens many times and each electron or positron emits Cherenkov light in the lead glass. Signals from these shower detectors were used for both energy and momentum measurements.

Along with the hodoscopes, the shower counters were used in particle tracking. The position measurements obtained from these two detector systems, together with the knowledge of the bending of the magnetic fields, allowed the reconstruction of particle paths, each of which corresponds to a specific particle momentum.

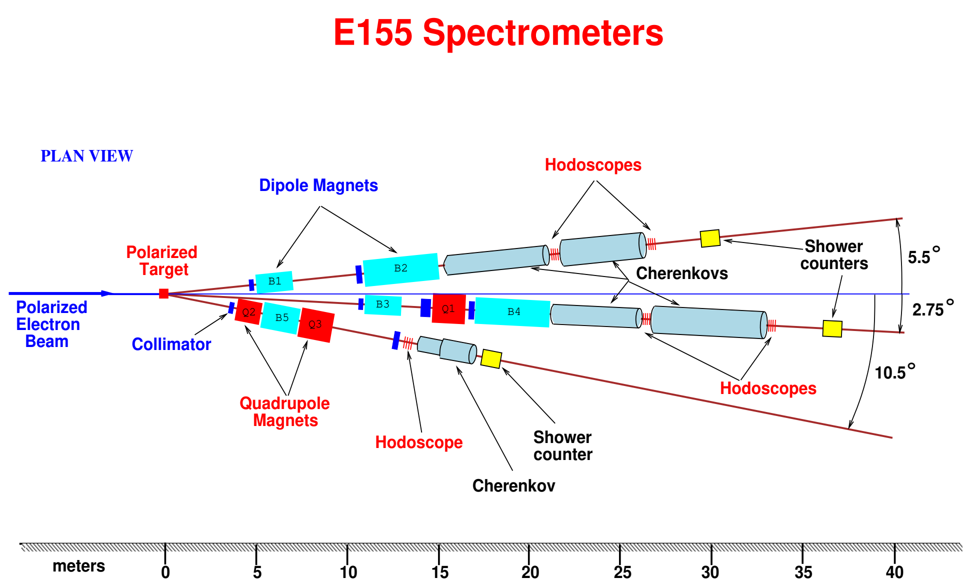

Figure 5: Layout of the Spectrometers for E155x

2.5 Experimental Asymmetries

The experimental asymmetries [15] were determined by the formula

$$A_{\perp} = \frac{C_1}{f P_t f_{RC} \cos\phi} \left\{ \left(\frac{N_L - N_R}{N_L + N_R} \right) \frac{1}{P_b} + A_{EW} \right\} + A_{RC} \tag{14}$$

where N_L and N_R are the rates for left and right beam helicity, corrected for pair-symmetric contributions (a few percent) and pions misidentified as electrons (a few

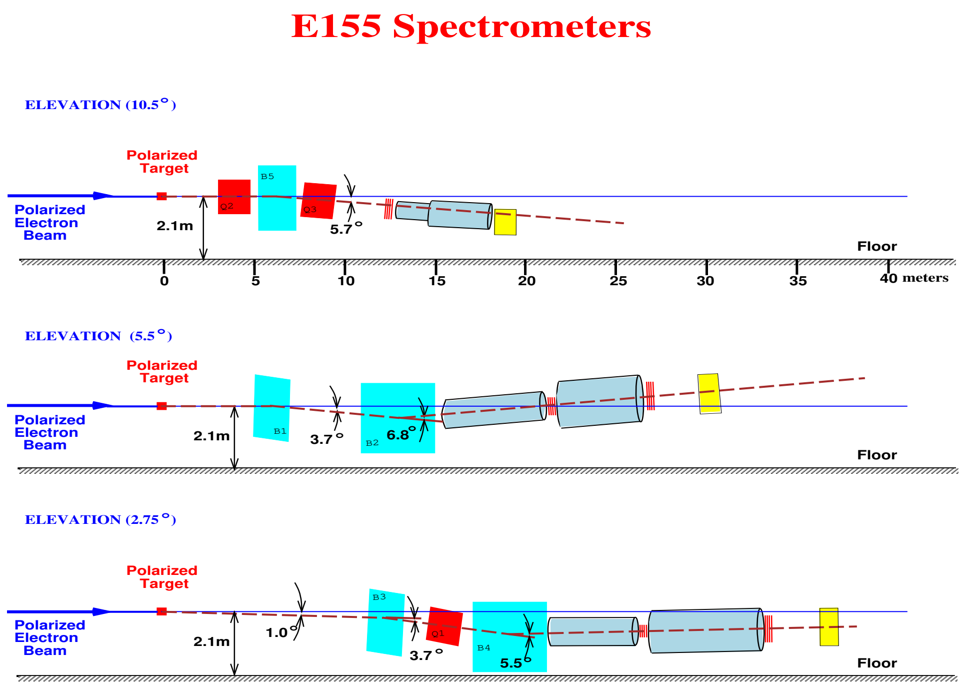

Figure 6: Side view of the Spectrometers for E155x

percent). The pair-symmetric contributions correct for the detection of non-deep-inelastically-scattered electrons, such as those produced in π^o decay. C_1 corrects for the unpolarized proton in ^{15}N and is approximately equal to 1. The angle between the plane that contains both the electron and proton spins vectors and the plane that contains both the incident and scattered electrons is given by ϕ. The dilution factor f represents the ratio of the number of polarizable protons or deuterons (i.e. np pairs) that electrons can scatter from to the total number of protons or deuterons present in the nucleus. For $^{15}NH_3$ $f \approx \frac{3}{15+3} \approx \frac{1}{6}$ and for ^{6}LiD $f \approx \frac{2}{2+2} \approx \frac{1}{2}$ (^{6}Li to a good approximation can be viewed as a polarizable deuteron and a non-polarizable alpha particle). A_{EW} is the electroweak asymmetry (calculated as a correction), P_b is the beam polarization (83%), and f_{RC} and A_{RC} take into account radiative corrections. Using the g_1 measurement from E155, one can obtain g_2 from Equation 8.

2.6 Preliminary Results

The preliminary results for A_2 and xg_2 from the SLAC analysis of E155x are shown in Figure 7. In general the new data are much more precise than those of previous experiments. The data for xg_2 follow g_2^{WW} very well. These results have been corrected for a constant electroweak asymmetry of value $A_{EW} = -8 \times 10^{-5} Q^2$. We can turn the analysis around and extract the electroweak asymmetry directly from these data.

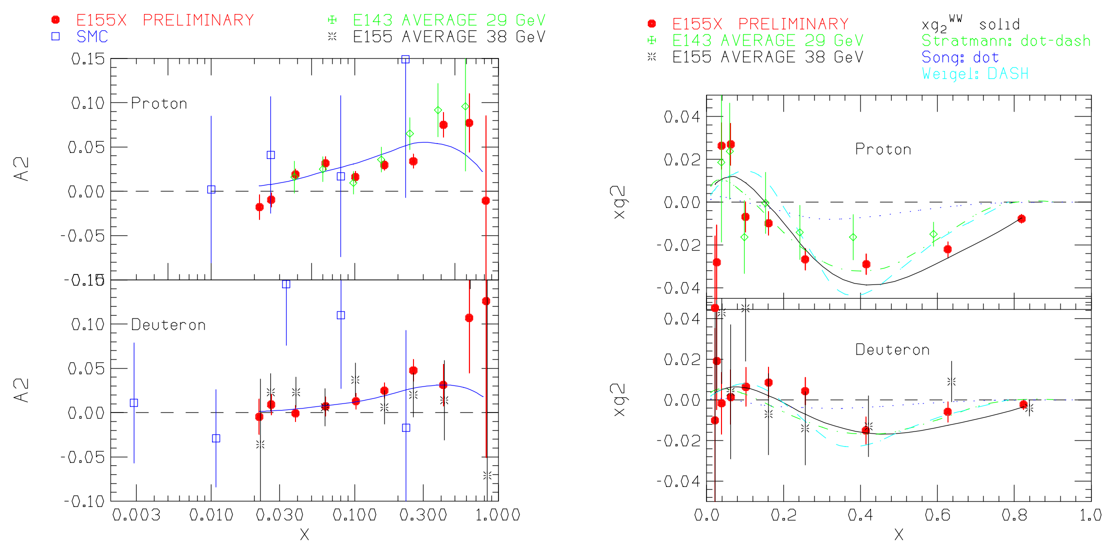

Figure 7: The plot on the left shows the preliminary results from E155x for A_2 as a function of x. The plot on the right shows the preliminary results from E155x for g_2.

3 The Electroweak Asymmetry

The perpendicular asymmetry $A_\perp$ contains a component of electroweak events. For an unpolarized target, the electroweak asymmetry is

$$A_{EW} = \frac{N_L - N_R}{N_L + N_R}, \tag{15}$$

where L and R refer to left and right beam helicities. Only the electroweak interaction breaks the symmetry between N_L and N_R. The parity violating electroweak asymmetry results from the interference between a single photon and a single Z^o exchange with the struck quark [13].

For a polarized target, the electromagnetic contribution changes sign when the target polarization is reversed, and therefore should cancel if there are equal amounts of data for both target polarizations. However, the electroweak asymmetry does not cancel. The raw asymmetries for the electromagnetic and electroweak interactions are $A_{EM} \approx 10^{-3}$ (for a single target polarization) and $A_{EW} \approx 10^{-4}$. Thus, the electroweak contribution is of significant size, and should be removed from $A_\perp$.

3.1 Theoretical Calculation of the Electroweak Asymmetry

The electroweak asymmetry for the proton is given by [18]

$$A_p^{EW} = \frac{3G_F Q^2}{\pi\alpha 2\sqrt{2}} \frac{2C_{1u}u(x) - C_{1d}[d(x) + s(x)] + Y[2C_{2u}u_v(x) - C_{2d}d_v(x)]}{4u(x) + d(x) + s(x)} \tag{16}$$

The up, down and strange quark distribution functions are described in terms of valence(v) and sea(s) contributions as

$$u(x) = u_v(x) + u_s(x) + \overline{u}_s(x)$$

$$d(x) = d_v(x) + d_s(x) + \overline{d}_s(x)$$

$$s(x) = s_s(x) + \overline{s}(x)$$

and it is assumed that the quark and antiquark sea distributions for each flavor are the same. Also, quarks heavier than the strange quark are neglected.

For the deuteron, the electroweak asymmetry is given by [18]

$$A_d^{EW} = \frac{3G_F Q^2}{\pi\alpha 2\sqrt{2}} \frac{2C_{1u} - C_{1d}[1 + R_s(x)] + Y(2C_{2u} - C_{2d})R_v}{5 + R_s(x)} \tag{17}$$

where

$$R_s(x) = \frac{2s(x)}{u(x) + d(x)} \quad \text{and} \quad R_v(x) = \frac{u_v(x) + d_v(x)}{u(x) + d(x)},$$

$$Y = \frac{1 - (1-y)^2}{1 + (1-y)^2 - y^2 R/(1+R)}$$

$$y = \frac{\nu}{E_o} \quad \text{and} \quad R = \frac{\sigma_L}{\sigma_T}$$

The variable y is termed the fractional energy transfer and is the ratio of the energy of the virtual photon to the beam energy. R is the ratio of longitudinal and transverse cross sections σ_L and σ_R . With $\sin^2\theta_w = 0.223$, the weak coupling coefficients are given by

$$C_{1u} = -\frac{1}{2} + \frac{4}{3}\sin^2\theta_w \approx -0.190$$
$$C_{1d} = \frac{1}{2} - \frac{2}{3}\sin^2\theta_w \approx 0.345$$
$$C_{2u} = -\frac{1}{2} + 2\sin^2\theta_w \approx -0.035$$
$$C_{2d} = \frac{1}{2} - 2\sin^2\theta_w \approx 0.035$$

A plot, shown in Figure 8, of A_p^{EW} and A_d^{EW} was generated using Equations 16 and 17. The CTEQ5M [17] distributions, a fit to the world's data for the quark distribution functions, were used in making the plots. Curves were generated for different strange quark distributions: normal, zero, and twice normal. Also plotted are preliminary data points for the electroweak asymmetry. These points were generated by assuming roughly equal left and right target polarization and adding the values of $A_\perp$ for each of these polarizations together in order to extract the electroweak asymmetry. Since $A_\perp$ contains both electromagnetic and electroweak terms, and the electromagnetic term is ten times that of the electroweak, erring in the amounts of left and right polarizations can cause large inaccuracies in the results. It can be seen that the differences between the three assumptions for the strange quark distribution (two of which are quite unlikely) are insignificant in comparison to the precision of the data. Since the strange quark distribution is least well known, this comparison is an assurance that the CTEQ5M results are accurate to far better than the level of our errors. It can also be seen that the data points, although having large errors, are compatible with the theoretical predictions. Improvement in these results was the main focus of the research reported herein.

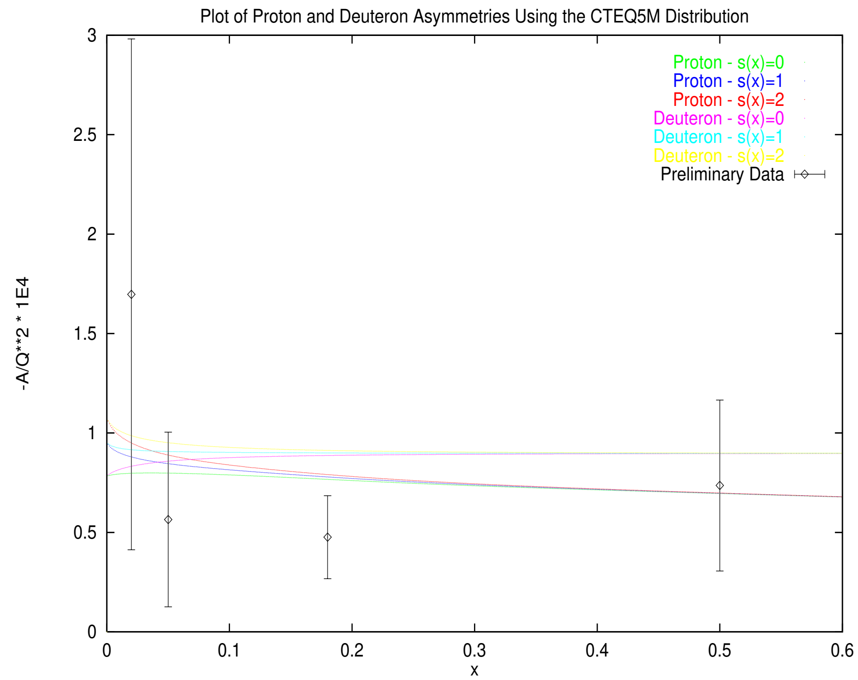

Figure 8: Plot of the theoretical predictions of electroweak asymmetry for the proton and deuteron and preliminary experimental results. The theoretical curves were generated using the CETEQ5M distributions for $s(x) = 0$, $s(x) =$ normal, and $s(x) = 2 \times$ normal. Note that the negative of the asymmetry is plotted.

3.2 Experimental Determination of the Electroweak Asymmetry

In the most general case, an asymmetry is defined as

$$A = \left(\frac{N_L - N_R}{N_L + N_R}\right) \tag{18}$$

where N_L and N_R respectively refer to the number of event originating from left and right handed electrons. Letting $N_L = N_L^{EM} + N_L^{EW}$ and $N_R = N_R^{EM} + N_R^{EW}$,

$$A = \frac{N_L^{EM} - N_R^{EM} + N_L^{EW} - N_R^{EW}}{N_L + N_R} \tag{19}$$

where $N_{L,R}^{EM,EW}$ are the number of electromagnetic and electroweak scattering events from left and right handed beam helicity. Since $N_{L,R}^{EW} << N_{L,R}^{EM}$, $N_L + N_R \approx N_L^{EM} + N_R^{EM}$, and thus,

$$A \approx \frac{N_L^{EM} - N_R^{EM}}{N_L^{EM} + N_R^{EM}} + \frac{N_L^{EW} - N_R^{EW}}{N_L + N_R}. \tag{20}$$

Defining

$$fP_tP_bA_\perp^{EM} \equiv \frac{N_L^{EM} - N_R^{EM}}{N_L^{EM} + N_R^{EM}} \quad \text{and} \quad A_{EW}P_b \equiv \frac{N_L^{EW} - N_R^{EW}}{N_L + N_R}, \tag{21}$$

we obtain

$$A_\perp^{meas} = \frac{N_L - N_R}{N_L + N_R}\left(\frac{1}{P_bP_tf}\right) = A^{EM} + A_{EW}\left(\frac{1}{fP_t}\right). \tag{22}$$

in which $A_\perp^{meas}$ is not corrected for electroweak events.

Weighted averages of a quantity Q were calculated using the statistical errors in $\sigma_i = \Delta A_\perp^{meas}$ for each run as:

$$< Q >= \frac{\sum_i Q_i/\sigma_i^2}{\sum_i 1/\sigma_i^2}. \tag{23}$$

Therefore,

$$A_\perp = \frac{\sum_i \left(A_{EM}^i + \frac{1}{(fP_t)^i}A_{EW}^i\right)/\sigma_i^2}{\sum_i \frac{1}{\sigma_i^2}} =< A_\perp^{EM} > + < \frac{1}{fP_t}A_{EW} > . \tag{24}$$

Since the run by run variations in fP_t, which depends only on target conditions, and the run by run fluctuations in A_{EW}, which depends only on counting statistics, are statistically independent, we can apply the relation

$$< Q_1Q_2 >=< Q_1 >< Q_2 > \tag{25}$$

to obtain

$$A_\perp^+ = A_\perp^{EM} + \ < \frac{1}{fP_t} >^+ A_{EW} \tag{26}$$

$$A_\perp^- = A_\perp^{EM} + \ < \frac{1}{fP_t} >^- A_{EW} \tag{27}$$

for positive and negative target polarization respectively. The term we call $< \frac{1}{fP_t} >$ is actually calculated as $< \frac{C_1}{fP_t\cos\phi} >$ in Equation 14. $< \frac{1}{fP_t} >$ can be either positive or negative depending on the the $\cos\phi$ term included in Equation 14 which is either ± 1.

Subtracting Equations 26 and 27 yields

$$A_\perp^+ - A_\perp^- =< \frac{1}{fP_t} >^+ A_{EW} - \ < \frac{1}{fP_t} >^- A_{EW} \tag{28}$$

and solving for A_{EW} yields

$$A_{EW} = \frac{A_{\perp}^{+} - A_{\perp}^{-}}{< \frac{1}{fP_t} >^{+} \; - \; < \frac{1}{fP_t} >^{-}}. \tag{29}$$

The error on the electroweak asymmetry is

$$\sigma_{EW} = \frac{\sqrt{\sigma_{+}^{2} \; + \; \sigma_{-}^{2}}}{| < \frac{1}{fP_t} >^{+} \; - \; < \frac{1}{fP_t} >^{-} |}. \tag{30}$$

Equations 29 and 30 will be used in the electroweak asymmetry calculation, in which $\sigma_{\pm}$ are the errors on $A^{\pm}$

4 Analysis and Results

4.1 Modification of the Analysis Code

In its original state, the analysis code used a value of $-0.00008Q^2$ for the electroweak contribution to $A_{\perp}$. In order to extract $A_{\perp}^{meas}$ the electroweak correction was set to 0. Also, the following product was calculated

$$\frac{fP_t \cos\phi}{C_1} \frac{P_b}{|P_b|}. \tag{31}$$

These variables are the same as those in Equation 14. The factor $\cos\phi$ has a value of -1 or 1 and corrects for the fact that the 2.75° and 10.5° spectrometers were on the opposite side of the beamline to the 5.5° spectrometer. The P_b and $\cos\phi$ terms only determined the sign, and the C_1 term was small enough to be absorbed into $< fP_T >$ as shown in the calculations above.

Each spectrometer was divided into 38 x bins and the asymmetry, as well as the product in Equation 31, was recorded for every bin in each of the three spectrometers for every run. Different cuts in the analysis, labeled #1 to # 20, were made to distinguish electrons from pions. A single electron definition, using optimal cuts to eliminate pions and other background, was selected for the output (#8 for the 2.75° and 5.5° and #11 for the 10.5° spectrometers). It was necessary to record the product in Equation 31 because the electroweak asymmetry, as given is Equation 14, depends on the average $< fP_t >$.

The extracted information was separated according to beam energy (29 or 32 GeV), target type (LiD or NH_3) and target polarization.

4.1.1 Comparison to Results Generated in the SLAC Analysis

It was necessary to check that results from this method of generating output from the analysis code compared well to previously generated results. Therefore, the electroweak correction of $-0.00008Q^2$ was turned back on and the resulting asymmetries from positive and negative target polarization were averaged. The comparison of these results and those results generated from the earlier analysis code, for a proton target and 29 GeV beam energy, is shown in Figure 9. It can be seen that the new results match extremely well with the earlier SLAC analysis conducted by Peter Bosted [19], thus giving some assurance that the new code for extracting asymmetries is working properly.

4.2 Grouping the Asymmetries by Bins

As stated previously, the data were extracted from the analysis code and printed out for each of the 38 x bins in each spectrometer for every run. The asymmetries and errors were averaged for each x bin in each spectrometer. In other words, there existed a list of 38 average asymmetries and errors for each of the three spectrometers.

4.2.1 Method of Finding Averages

To find the average asymmetry for each bin, the following formula was used

$$A_\perp = \frac{\sum_i \left(\frac{1}{\Delta A_\perp^i}\right)^2 A_\perp^i}{\sum_i \left(\frac{1}{\Delta A_\perp^i}\right)^2} \qquad (32)$$

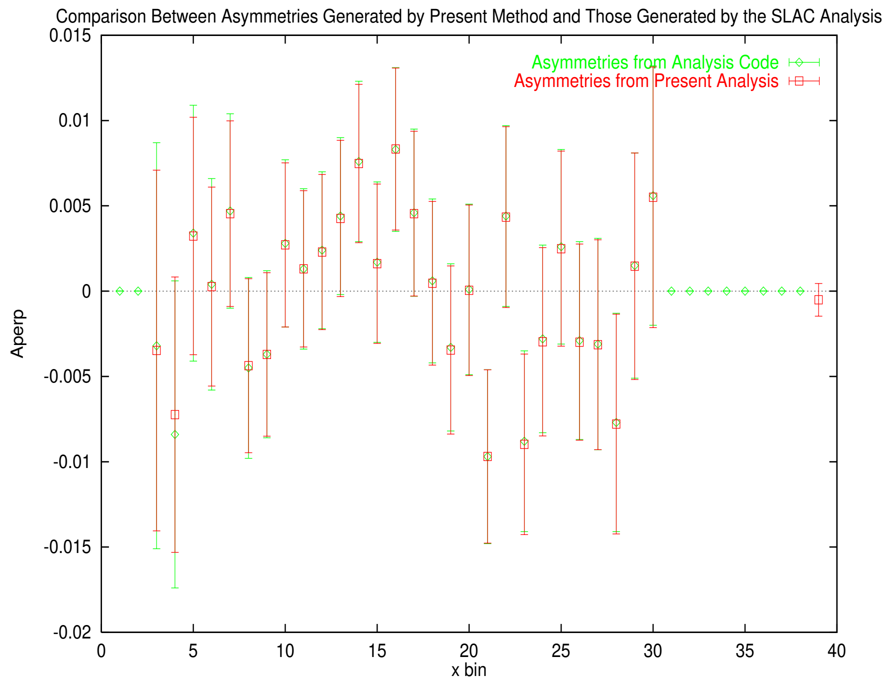

Figure 9: Comparison to the asymmetries generated in the SLAC analysis. Results are shown for averaged positive and negative target polarization, 29 GeV beam energy, and a proton target.

where $A_{\perp}^{i}$ and the error $\Delta A_{\perp}^{i}$ for each run are averaged. The error was found by using

$$\Delta A_{\perp} = \frac{1}{\sqrt{\sum_i \left(\frac{1}{\Delta A_{\perp}^{i}}\right)^2}} \tag{33}$$

This method of determining weighted averages was used throughout the analysis when combining asymmetries and errors.

4.3 Scaling the Asymmetries and Errors

The averages and errors generated for each bin in x were scaled by the appropriate $< Q^2 >$, which was obtained from the weighted average of all events in a particular bin. The values of $< Q^2 >$ were specific to each x bin.

4.4 Adding the Positive and Negative Values

For each x bin, the scaled values for positive and negative target polarization were combined to obtain an electroweak asymmetry. Equations 29 and 30 were used to find the electroweak asymmetry and its error.

4.5 Weighted Averages in x

The 38 x bins were reduced to only four in Bjorken x using a weighted average. In addition, the results for the two energies and the three spectrometers were combined so there existed a single electroweak asymmetry for each Bjorken x bin for both positive and negative target polarizations. The results of this averaging and combination are shown in Figure 10. The theoretical curves generated using the CETEQ5M quark distributions are also plotted in Figure 10. The deuteron curve in its original form was used for the LiD target. For the $^{15}NH_3$ target the following combination of curves was used: $\frac{4}{18}A^p_{EW} + \frac{14}{18}A^d_{EW}$. This combination was necessary because the ammonia target consists of four protons and 14 deuterons.

The results were also compared to the preliminary results which were generated by assuming equal amounts of target polarization (Figure 8). This comparison is shown in Figure 11. It can be seen that the results from the final analysis are consistent with those from the earlier analysis and have slightly better statistics.

The asymmetries for each target were then averaged to give a single value for each x bin (see Figure 12). Finally these four x bin results were averaged to give a final value for the electroweak asymmetry (Figure 13) evaluated at the properly weighted average of Bjorken x.

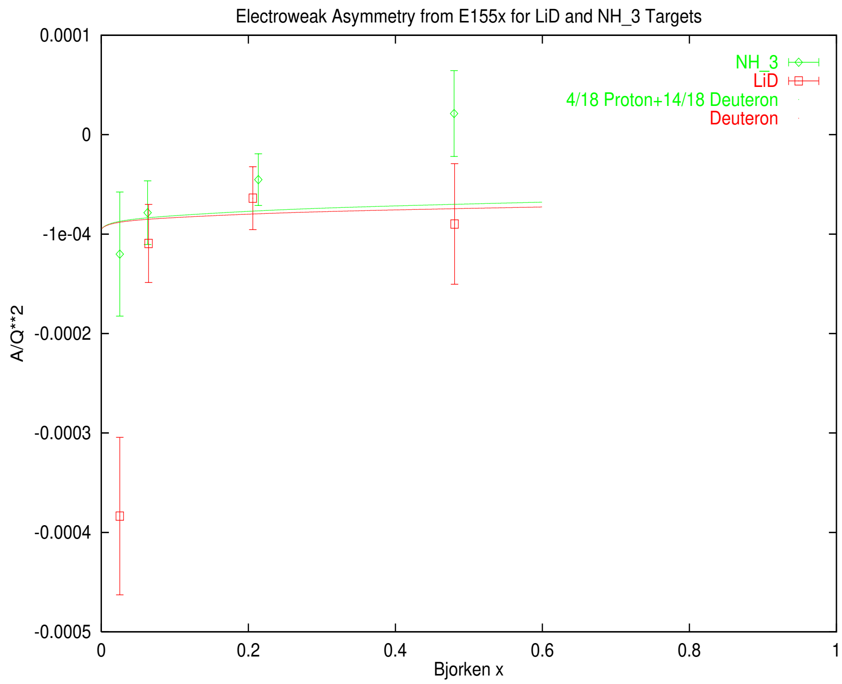

Figure 10: Experimental asymmetries for both LiD and $^{15}NH_3$ targets as well as the theoretical curves generated by the CETEQ5M quark distributions.

5 Conclusions

The final value of the electroweak asymmetry measured in E155x is

$$A_{EW} = (-7.19 \times 10^{-5} \pm 1.37 \times 10^{-5})Q^2 \tag{34}$$

This result agrees with the theoretical expectations. As Figure 13 shows, the line generated with the CETEQ5M distribution passes through the result given by Equation 34. The theoretical curve gives a value of $-7.88 \times 10^{-5}Q^2$ at $x = 0.192$, the position where the average measured asymmetry is located. Since this curve is almost linear, this value can be used for the overall theoretical average. Also, the value used to correct the g_2 results, $-8 \times 10^{-5}Q^2$, is within the error bars of the result reported in this work.

The result reported herein also allows for the conclusion that the “false” asymme-

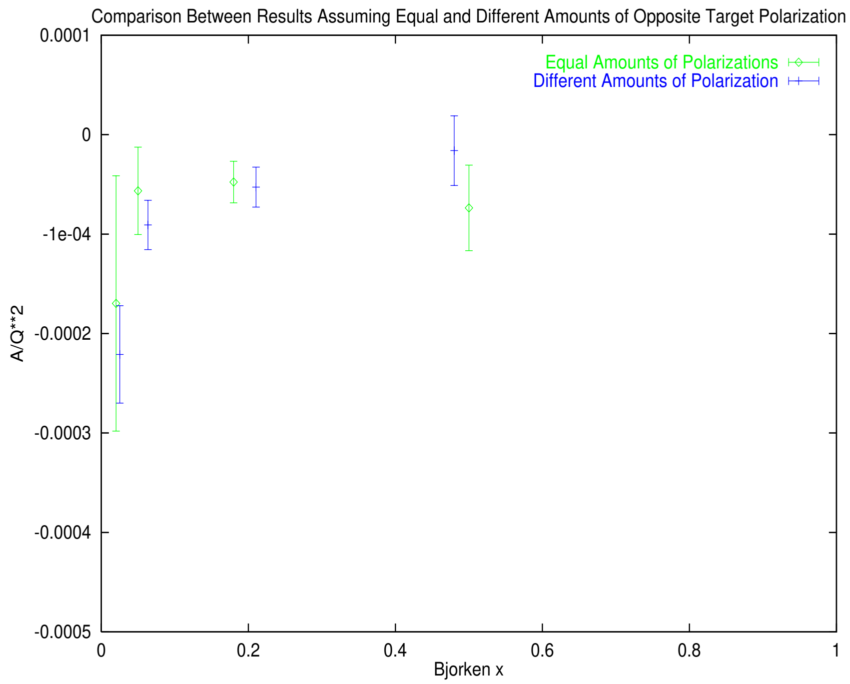

Figure 11: Comparison between experimental electroweak asymmetries generated assuming the data contained equal amounts of opposite target polarizations (the early results shown in Figure 8) and electroweak asymmetries generated by accounting for slightly different amounts of opposite target polarization. (Figure 10 results averaged over target materials.)

tries in the experiment are on the level of

$$|7.19 \times 10^{-5} - 7.88 \times 10^{-5}| = 6.9 \times 10^{-6}. \tag{35}$$

False asymmetries are generated by any small systematic differences between opposite beam polarizations that are unrelated to the physics of the experiment. For example, the beam might travel along a slightly different path for different polarizations. The present results show that the false asymmetries are less than 1% of the typical value of $A_\perp$ and therefore of little import with respect to their contribution to the g_2 measurement.

In addition, A_{EW} calculated assuming equal amounts of run time with left and right target polarizations is given by

$$A_{EW} = \frac{1}{2}\left[A_\perp^+ < fP_t > + A_\perp^- < fP_t >\right], \tag{36}$$

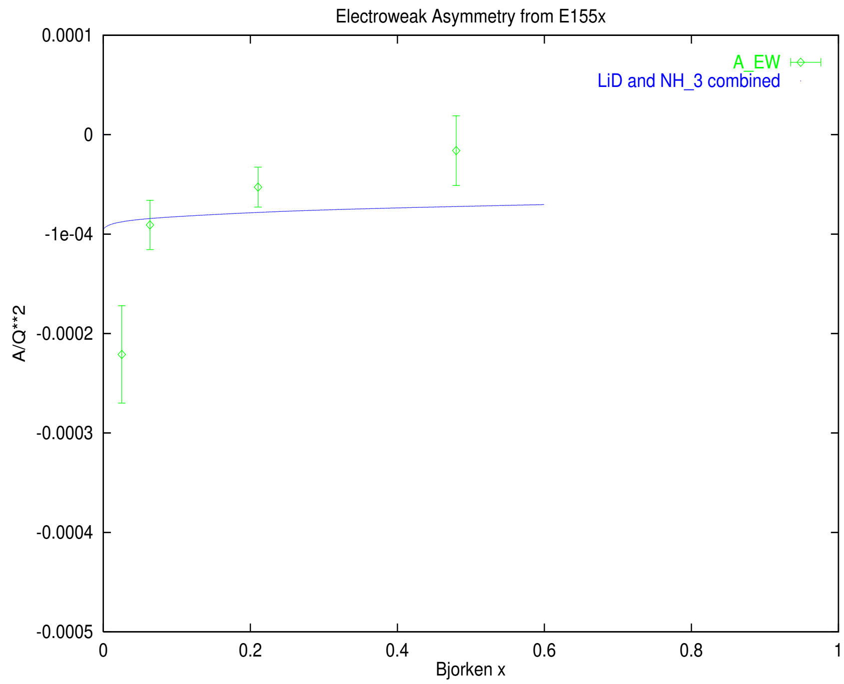

Figure 12: The electroweak asymmetry over four bins in x. Also shown is the average theoretical curve for the NH_3 and LiD targets.

with the following result:

$$A_{EW} = (-7.33 \times 10^{-5} \pm 1.39 \times 10^{-5})Q^2 \tag{37}$$

This compares well with the result which accounted for different amounts of target polarization (Equation 34) and allows for the conclusion that the difference between amounts of opposite target polarization was very small.

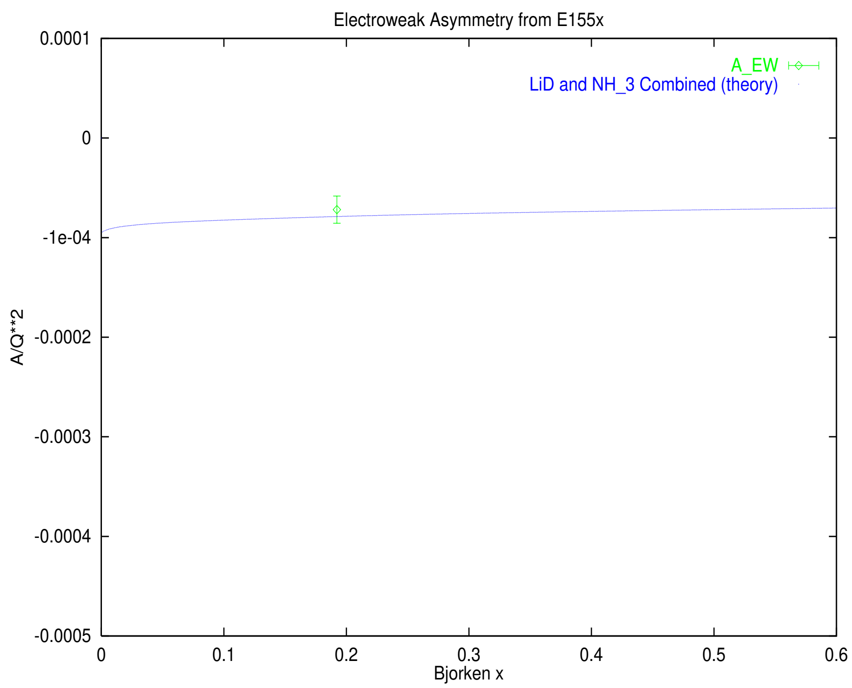

Figure 13: The Electroweak asymmetry averaged over x bins. Also shown is the average theoretical curve for the NH_3 and LiD targets using the CETEQ5M quark distributions. The value for the data point is $-0.0000719 \pm 0.00000137$ at $x = 0.192$

6 Tables of Results

Table 2: Value averaged over four bins in x for separate target polarizations and target types

Polarization	Target	Bin	$< x >$	$< Q^2 >$	$A_\perp^{meas}$	$\Delta A_\perp$
$-$	LiD	1	0.0233323	0.8429978	0.0044151	0.0030871
		2	0.0638046	1.5017358	0.0021633	0.0021343
		3	0.1892825	3.1877837	0.0006640	0.0022467
		4	0.4766562	7.1827556	-0.0197585	0.0085528
	NH_3	1	0.0232572	0.8454089	0.0003600	0.0018642
		2	0.0633156	1.4870013	0.0023831	0.0013287
		3	0.1923955	3.1753302	-0.0024246	0.0013771
		4	0.4830315	7.3245904	-0.0284834	0.0047061
$+$	LiD	1	0.0233503	0.8340932	-0.0086018	0.0031121
		2	0.0638688	1.4785886	-0.0018465	0.0021452
		3	0.1892192	3.1277721	-0.0017860	0.0022525
		4	0.4778486	7.0313856	-0.0041773	0.0084659
	NH_3	1	0.0232964	0.8439092	-0.0022961	0.0018851
		2	0.0633764	1.4814540	0.0021355	0.0013354
		3	0.1924094	3.1580557	-0.0065302	0.0013775
		4	0.4825868	7.3191291	-0.0290878	0.0047329

Table 3: Values of $< \frac{1}{fP_t} >$ for each target polarization, beam energy, target type, and spectrometer averaged over x

Targer Polarization	Beam Energy	Target	Spect. 1	Spect. 2	Spect. 3
$-$	29	LiD	12.4205	-12.1631	12.2201
		NH_3	10.1149	-10.0308	9.2400
	32	LiD	-14.0650	13.8375	-13.521
		NH_3	-10.3057	10.0759	-9.8570
$+$	29	LiD	-13.8619	13.5541	-13.8093
		NH_3	-10.8405	10.5953	-10.3640
	32	LiD	13.8174	-13.5126	13.1861
		NH_3	10.2901	-10.0911	9.8337

Table 4: Values of A_{EW} for different target types

Target	Bin	x	A_{EW}	ΔA_{EW}
LiD	1	0.0251900	-0.0003836	0.0000792
	2	0.0642371	-0.0001094	0.0000393
	3	0.2060890	-0.0000639	0.0000316
	4	0.4804518	-0.0000898	0.0000606
NH_3	1	0.0251741	-0.0001201	0.0000624
	2	0.0629128	-0.0000785	0.0000320
	3	0.2135480	-0.0000452	0.0000260
	4	0.4798768	0.0000212	0.0000431

Appendices

The following appendices contain the code to produce the theoretical plots using the CTEQ5M quark distributions, modifications to *analsum.f*, the main analysis code used to extract the information necessary to calculate the electroweak asymmetry, along with the perl code used to analyze the output from *analsum.f*.

A Code to generate theoretical plots

```
// ***************************************************************************
// * asym.cc *
// Calculates the value of A
// Sept 29, 1999
// ***************************************************************************


#include <fstream.h>
#include <stdlib.h>
#include <math.h>

// function prototypes
double C( int, char );                                  //
double Y(double,double);                                //
double quark(char, char, double, double);               // quark distributions
double R_s(double, double);                             // for deuteron
double R_v(double, double);                             // for deuteron
extern "C" void r1998_(double*,double*,double*,double*,int*);
extern "C" double ctq5pdf_(long *, double*, double*);
extern "C" void setctq5_(long *);

// declarationsy
double ALPHA = 0.00729927;                // fine structure constant
const double Gf=1.16639e-5;               // coupling constants
double A_P;                               // proton asymmetery
double A_D;                               // dueteron asymmetry
double y = 1;                             // y = nu/E = (E-E')/E
double R = 0.1;                           // R = sigma_L/sigma_T
const double PI = 3.141;                  // Pi
char up = 'u';                            // for up quark
char down = 'd';                          // for down quark
char strange = 's';                       // for strange quark
char none = 'n';                          // no subscript
char subv = 'v';                          // subscript of v

double SD = 1;                            // strange quark distribution factor



int main(int argc, char *argv[])
{
  //************************************************************************
  // Check command line arguments
  if( argc < 5 ){
    cout << "Usage: asym x Q2 BeamEnergy Fit# [-v]\n" << endl;
    exit(1);
  } //if
```

```
int VERBOSE = 0;                          // verbose mode is initially off
double X = atof(*++argv);                        // bjorken x
argc--;
double Q2 = atof(*++argv);                        // Q^2 momentum transfer
argc--;
double Energy = atof(*++argv);                   // Beam energy
argc--;
long Fit = atoi(*++argv);
argc--;
setctq5_(&Fit);

cout << "X = " << X << endl;
cout << "Q2 = " << Q2 << endl;
cout << "Energy = " << Energy << endl;

while( (argc > 1) && (argv[1][0] == '-') ){
  switch( argv[1][1] ){
  case 'v':
    VERBOSE = 1;                          // set verbose mode
    break;
  default:
    break;
  } // switch
  ++argv;
  --argc;
} //while

cout << "VERBOSE = " << VERBOSE << endl;
//**********************************************************************

// The program
// declarations
//  double ALPHA = 0.007299;                  // fine structure constant
//const double Gf=1.16639e-5;               // coupling constants
//double A_P;                               // proton asymmetery
//  double A_D;                               // dueteron asymmetry
//double y = 1;                             // y = nu/E = (E-E')/E
//double R = 0.1;                           // R = sigma_L/sigma_T
//const double PI = 3.141;                  // Pi
//char up = 'u';                            // for up quark
// char down = 'd';                          // for down quark
//char strange = 's';                       // for strange quark
//char none = 'n';                          // no subscript
//char subv = 'v';                          // subscript of v
// formula for A

cout << "C(1,up) = " << C(1,up) << endl;
cout << "C(1,down) = " << C(1,down) << endl;
cout << "C(2,up) = " <<C(2,up) << endl;
cout << "C(2.down) = " << C(2,down) << endl;
cout << "Y = " << Y(1,0.1) << endl;
cout << "u = " << quark(up,none,X,Q2) << endl;
cout << "u_v = " << quark(up,subv,X,Q2) << endl;
cout << "d = " << quark(down,none,X,Q2) << endl;
cout << "d_v = " << quark(down,subv,X,Q2) << endl;
cout << "s = " << quark(strange,none,X,Q2) << endl;

double dR;
int goodfit;
```

```
  r1998_(&X,&Q2,&R,&dR,&goodfit);
  cout << "R = " << R << endl;

  A_P = ( (3*Gf*Q2) / (PI*ALPHA*2*sqrt(2)) ) *
  ( 2*C(1,up)*quark(up,none,X,Q2) - C(1,down)*(quark(down,none,X,Q2)+
  SD*quark(strange,none,X,Q2)) + Y(y,R) * (2*C(2,up)*quark(up,subv,X,Q2) -
  C(2,down)*quark(down,subv,X,Q2)) ) / ( 4*quark(up,none,X,Q2) +
  quark(down,none,X,Q2) + SD*quark(strange,none,X,Q2) );

  A_D = ( (3*Gf*Q2) / (PI*ALPHA*2*sqrt(2)) ) *
  ( 2*C(1,up) - C(1,down)*(1+ R_s(X,Q2)) + Y(y,R) * (2*C(2,up) -
  C(2,down))*R_v(X,Q2) ) / ( 5 + R_s(X,Q2) );

  //A_D = (3*Gf*Q2)/(PI*ALPHA*2*sqrt(2)) * ( 2*C(1,up) - C(1,down)*(1+R_s(X,Q2))
          + Y(y,R)*(2*C(2,up) - C(2,down))*R_v(X,Q2) ) / (5 + R_s(X,Q2));

  double test;
  test = -0.0001*Q2*(0.77*(1+0.44*R_s(X,Q2)) + 0.11*Y(y,R));
  cout << "test = " << test << endl;

  if (VERBOSE == 0) cout << A_P << "\n" << A_D  << endl;
  else cout << X << " " << Q2 << " " << Energy << " " << A_P << " " << A_D << endl;
} // main


// ************************************************************************************
// double C( int subscript, char direction );
// Calcualates the value of C_subscript_direction for theta_w angle
// ************************************************************************************
double C( int subscript, char direction )
{
  if( (subscript==1) && (direction=='u') )      return(-0.190);
  else if( (subscript==1) && (direction=='d') ) return(0.345);
  else if( (subscript==2) && (direction=='u') ) return(-0.035);
  else if( (subscript==2) && (direction=='d') ) return(0.035);
} // C

// *************************************************************************************
// double Y(double y, double R)
// Calculates Y as a function of y= nu/E= (E-E')/E and R=sigma_L/sigma_T
// *************************************************************************************
double Y(double y, double R)
{
  double value;
  value = (1 - (1-y)*(1-y)) / ( 1 + (1-y)*(1-y) -y*y*R/(1+R) );
  return(value);
} // Y

// **************************************************************************************
// double quark(char label, char subscript, double X);
// Calculates the  quark distribution q(x) = q_v(x) + q_s(x) for up, down, strange
// **************************************************************************************
double quark(char label, char subscript, double X, double Q2)
{
  long iparton, iparton1;
  double q = sqrt(Q2);
//  double ctq5pdf_(long *, double *, double *);

  if( label=='u' ){
```

```
    iparton = 1;
    iparton1 = -1;
    cout << ctq5pdf_(&iparton,&X,&q) << endl;
    if( subscript=='v' ) return(ctq5pdf_(&iparton,&X,&q)-ctq5pdf_(&iparton1,&X,&q));
 //   else if( subscript=='n' ) return(1);
    else if( subscript=='n' ) return(ctq5pdf_(&iparton,&X,&q));
    else exit(1);
  } //if u
  if( label=='d' ){
    iparton = 2;
    iparton1 = -2;
    if( subscript=='v' ) return(ctq5pdf_(&iparton,&X,&q)-ctq5pdf_(&iparton1,&X,&q));
    else if( subscript=='n' ) return(ctq5pdf_(&iparton,&X,&q));
    else exit(1);
  } //if d
  if( label=='s' ){
    iparton = 3;
    if( subscript=='n' ) return(ctq5pdf_(&iparton,&X,&q));
    else exit(1);
  } //if s
} //quark

// ********************************************************************************************
// double R_s(double X, double Q2)
// For deuteron
// ********************************************************************************************
double R_s(double X, double Q2)
{
 double value;
 value = (SD * 2*quark(strange,none,X,Q2) ) / ( quark(up,none,X,Q2) + quark(down,none,X,Q2) );
 return(value);
} // R_s

// ********************************************************************************************
// double R_v(double X, double Q2)
// For deuteron
// ********************************************************************************************
double R_v(double X, double Q2)
{
 double value;
 value = ( quark(up,subv,X,Q2) + quark(down,subv,X,Q2) ) /
   ( quark(up,none,X,Q2) + quark(down,none,X,Q2) );
 return(value);
} // R_s
```

B Modifications to *analsum.f*

```
C Applyq EW corr. Use + for 29 GeV, - for 32 gev. Only for elec. defs.
C*** set EW correction to 0 2/1/00
            if(ie.eq.1.and.ipth.le.14) asy(i,j,k)=asy(i,j,k)
     >       -0.00000*q2sv(i,j,ie)*beampol
            if(ie.eq.2.and.ipth.le.14) asy(i,j,k)=asy(i,j,k)
     >       +0.00000*q2sv(i,j,ie)*beampol


!!!!!!!!!!!!!!!!!!!!!!!!!!!!!!!!!!!!!!!!!!!!!!!!!!!!!!!!!!!!!!!!!!!!!!!
! Added 3/3/00 for electroweak asymmetry
            EWSTUFF = DILUTION*c1*(TARGPOL(rn,1)/100.)
     >                *BEAMSIGN/APERPCOR
!!!!!!!!!!!!!!!!!!!!!!!!!!!!!!!!!!!!!!!!!!!!!!!!!!!!!!!!!!!!!!!!!!!!!!!!


!!!!!!!!!!!!!!!!!!!!!!!!!!!!!!!!!!!!!!!!!!!!!!!!!!!!!!!!!!!!!!!!!!!!!!!!!
! Added to print out info for each spectrometer                         !
!!!!!!!!!!!!!!!!!!!!!!!!!!!!!!!!!!!!!!!!!!!!!!!!!!!!!!!!!!!!!!!!!!!!!!!!!
              ! Spectrometer 1
              IF(j.eq.1.and.ipth.eq.8) THEN
                 WRITE(50, '(i4, i3, i2, i3, f10.4, f8.3, f10.4,f10.4,
     >                 f8.3, f8.3, f8.3, f8.3, i2, i2 )')
     >                rn, i, j, IPTH, ASY(I,J,K), ASYER(I,J,K),
     >                EWSTUFF, (TARGPOL(rn,1)/100.),DILUTION,c1,
     >                BEAMSIGN, APERPCOR, IE, IT
!                PRINT"(i4, f10.5)",rn, TARGPOL(rn,1)
!                PRINT"(i4, f10.5)",rn,TARGNUM(rn)
              ENDIF

              ! Spectrometer 2
              IF(j.eq.2.and.ipth.eq.8) THEN
                 WRITE(51, '(i4, i3, i2, i3, f10.4, f8.3, f10.4,f10.4,
     >                 f8.3, f8.3, f8.3, f8.3, i2, i2)')
     >                rn, i, j, IPTH, ASY(I,J,K), ASYER(I,J,K),
     >                EWSTUFF, (TARGPOL(rn,1)/100.), DILUTION,c1,
     >                BEAMSIGN, APERPCOR, IE, IT
              ENDIF

              !Spectrometer 3
              IF(j.eq.3.and.ipth.eq.11) THEN
                 WRITE(52, '(i4, i3, i2, i3, f10.4, f8.3, f10.4,f10.4,
     >                 f8.3, f8.3, f8.3, f8.3, i2, i2)')
     >                rn, i, j, IPTH, ASY(I,J,K), ASYER(I,J,K),
     >                EWSTUFF, (TARGPOL(rn,1)/100.), DILUTION,c1,
     >                BEAMSIGN, APERPCOR, IE, IT
              ENDIF
!!!!!!!!!!!!!!!!!!!!!!!!!!!!!!!!!!!!!!!!!!!!!!!!!!!!!!!!!!!!!!!!!!!!!!!!!!!


!!!!!!!!!!!!!!!!!!!!!!!!!!!!!!!!!!!!!!!!!!!!!!!!!!!!!!!!!!!!!!!!!!!!!!!!!!
! Added 3/25/00 to try to match peter's results
              IF(j.eq.1.and.IPTH.eq.8.and.IT.eq.1) THEN
                WRITE(53,'(i4,i3,i2,i3,f10.4,f10.4)')
     >            rn,i,j,IPTH,ASY(I,J,K),ASYER(I,J,K)
              ENDIF
!!!!!!!!!!!!!!!!!!!!!!!!!!!!!!!!!!!!!!!!!!!!!!!!!!!!!!!!!!!!!!!!!!!!!!!!!!
```

C Code to Group Averages by Bin

```
#! /usr/local/bin/perl

################################################################################
# average.pl
# Takes the output from asyrun_*.dat generated by analsum and groups the
# average perpendicuar asymetry and error by bin number
#
# For new analysis, averages more than A,err,ewstuff
#
# Usage: average.pl spectrometer_number
################################################################################

# Get Spectrometer Number
if ($#ARGV == 0){
    $spect = shift @ARGV;
} # if
else{
    die "Usage: average.pl spectrometer_number\n";
} # else

# Radial cut (IPTH) to be used
if( ($spect == 1) || ($spect == 2) ){
    $ipth = 8;
} #if
elsif( ($spect == 3) ) {
    $ipth = 11;
} #elsif
else{
    die "Spectrometer number must be 1, 2, or 3\n";
} #else

#define columns in asyrun.out
$c_run = 0;                         # run number   (rn)
$c_bin = 1;                         # bin number   (i)
$c_spect = 2;                       # spectrometer (j)
$c_ipth = 3;                        # radial cut (ipth)
$c_asy = 4;                         # the asymetery
$c_err = 5;                         # the error in the asymetery
$c_ewstuff = 6;                     # the constants for ew asymmetry
$c_targpol = 7;                     # target polarization
$c_dilution = 8;                    # dilution factor
$c_c1 = 9;                          # c1
$c_beamsign = 10;                   # beamsign
$c_aperpcor = 11;                   # aperp correction
$c_ie = 12;                         # beam energy (29 or 32)
$c_it = 13;

open( IN_POS29LI, "../asyrun_pos_29_li_$spect.dat") || die "1could not open asyrun_$spect.dat\n";
open( IN_NEG29LI, "../asyrun_neg_29_li_$spect.dat") || die "2could not open asyrun_$spect.dat\n";
open( IN_POS32LI, "../asyrun_pos_32_li_$spect.dat") || die "3could not open asyrun_$spect.dat\n";
open( IN_NEG32LI, "../asyrun_neg_32_li_$spect.dat") || die "4could not open asyrun_$spect.dat\n";

open( IN_POS29NH, "../asyrun_pos_29_nh_$spect.dat") || die "5could not open asyrun_$spect.dat\n";
open( IN_NEG29NH, "../asyrun_neg_29_nh_$spect.dat") || die "6could not open asyrun_$spect.dat\n";
open( IN_POS32NH, "../asyrun_pos_32_nh_$spect.dat") || die "7could not open asyrun_$spect.dat\n";
open( IN_NEG32NH, "../asyrun_neg_32_nh_$spect.dat") || die "8could not open asyrun_$spect.dat\n";
```

```
open( OUT_POS29LI, ">asybin_pos_29_li_$spect.out")  || die "could not open asybin_$spect.out\n";
open( OUT_NEG29LI, ">asybin_neg_29_li_$spect.out")  || die "could not open asybin_$spect.out\n";
open( OUT_POS32LI, ">asybin_pos_32_li_$spect.out")  || die "could not open asybin_$spect.out\n";
open( OUT_NEG32LI, ">asybin_neg_32_li_$spect.out")  || die "could not open asybin_$spect.out\n";

open( OUT_POS29NH, ">asybin_pos_29_nh_$spect.out")  || die "could not open asybin_$spect.out\n";
open( OUT_NEG29NH, ">asybin_neg_29_nh_$spect.out")  || die "could not open asybin_$spect.out\n";
open( OUT_POS32NH, ">asybin_pos_32_nh_$spect.out")  || die "could not open asybin_$spect.out\n";
open( OUT_NEG32NH, ">asybin_neg_32_nh_$spect.out")  || die "could not open asybin_$spect.out\n";

for( $k=0; $k<8; $k++ ){                          # do for both positive and negavite
    if( $k==0 ){
$INFILE = "IN_POS29LI";
$OUTFILE = "OUT_POS29LI";
    } #if
     if( $k==1 ){
$INFILE = "IN_POS29NH";
$OUTFILE = "OUT_POS29NH";
    } #if
    elsif( $k==2 ){
$INFILE = "IN_NEG29LI";
$OUTFILE = "OUT_NEG29LI";
    } #if
    elsif( $k==3 ){
$INFILE = "IN_NEG29NH";
$OUTFILE = "OUT_NEG29NH";
    } #i
    elsif( $k==4 ){
$INFILE = "IN_POS32LI";
$OUTFILE = "OUT_POS32LI";
    } #if
    elsif( $k==5 ){
$INFILE = "IN_POS32NH";
$OUTFILE = "OUT_POS32NH";
    } #if
    elsif( $k==6 ){
$INFILE = "IN_NEG32LI";
$OUTFILE = "OUT_NEG32LI";
    } #if
    elsif( $k==7 ){
$INFILE = "IN_NEG32NH";
$OUTFILE = "OUT_NEG32NH";
    } #if



    # Reset variables;
    for( $i=1; $i<=39; $i++ ){
$avg_num[$i] = 0;
$avg_dem[$i] = 0;
$avg_ewstuff[$i] = 0;
$avg_invewstuff[$i] = 0;
    } #for

    while( <$INFILE> ){
@line = split(/\s+/,$_);
$bin = $line[$c_bin];
if($line[$c_ipth] != $ipth){next};         # pick out a radial cut
if($line[$c_err] == 0){next};              # exclude bad points
```

```
if($line[$c_spect] != $spect){next};       # pick out current spect
if($line[$c_targpol] == 1.0){next};        # ignore mollar runs

$avg_num[$bin] += $line[$c_asy]*(1/$line[$c_err])**2;
$avg_dem[$bin] += (1/$line[$c_err])**2;
$avg_ewstuff[$bin] += $line[$c_ewstuff]*(1/$line[$c_err])**2;
$avg_invewstuff[$bin] += (1/$line[$c_ewstuff])*(1/$line[$c_err])**2;
    } #while

    for( $i=1; $i<=39; $i++ ){                            # get info for each bin
if($avg_dem[$i] == 0){next};
$asy[$i] = $avg_num[$i]/$avg_dem[$i];
$err[$i] = 1/($avg_dem[$i])**(1/2);
$ew[$i] = $avg_ewstuff[$i]/$avg_dem[$i];
$invew[$i] = $avg_invewstuff[$i]/$avg_dem[$i];

printf $OUTFILE "%1s %10.5f %10.5f %10.5f %10.5f\n", $i, $asy[$i], $err[$i], $ew[$i],$invew[$i];
    } #for


    close($INFILE) || die "Can not close asybin_$spect.dat\n";
    close($OUTFILE) || die "Can not close asybin_$spect.dat\n";

} #for
```

D Code to Scale the Results by Q^2

```
#! /usr/local/bin/perl

######################################################################
# divide_q2.pl
# Divides the ewstuff and the error by the appropriate Q2
# Outputs to div* files
######################################################################
$c_bin = 0;
$c_asy = 1;
$c_err = 2;
$c_ew = 3;
$c_q2 = 1;
$c_ewinv = 4;

foreach $energy (29,32){
    foreach $targtype ("li","nh"){
foreach $spect (1,2,3){

    open( INPOS, "asybin_pos\_$energy\_$targtype\_$spect.out" ) || die "bad input1\n";;
    open( INNEG, "asybin_neg\_$energy\_$targtype\_$spect.out" ) || die "bad input2\n";
    open( INQ2,  "q2\_$energy\_$targtype\_$spect.out" )         || die "bad q2\n";
    open( OUTPOS, ">div_pos\_$energy\_$targtype\_$spect.out" )  || die "bad output1\n";
            open( OUTNEG, ">div_neg\_$energy\_$targtype\_$spect.out" )  || die "bad output1\n";

    while(<INPOS>){
@line = split(/\s+/,$_);
$bin = $line[$c_bin];
$asy_pos[$bin] = $line[$c_asy];
$err_pos[$bin] = $line[$c_err];
$ew_pos[$bin] = $line[$c_ew];
$ewinv_pos[$bin] = $line[$c_ewinv];
    } #while

    while(<INNEG>){
@line = split(/\s+/,$_);
$bin = $line[$c_bin];
$asy_neg[$bin] = $line[$c_asy];
$err_neg[$bin] = $line[$c_err];
$ew_neg[$bin] = $line[$c_ew];
$ewinv_neg[$bin] = $line[$c_ewinv];
    } #while

    while(<INQ2>){
@line = split(/\s+/,$_);
$bin = $line[$c_bin];
$q2[$bin] = $line[$c_q2];
    } #while

    for($i=1;$i<39;$i++){
if( $energy == 29 ){
    $pos_ew_asy[$i] = +1*$asy_pos[$i]/$q2[$i];
    $neg_ew_asy[$i] = +1*$asy_neg[$i]/$q2[$i];
} #if
elsif( $energy == 32 ){
    $pos_ew_asy[$i] = $asy_pos[$i]/$q2[$i];
    $neg_ew_asy[$i] = $asy_neg[$i]/$q2[$i];
} #if
```

```
$pos_ew_asy_err[$i] = $err_pos[$i]/$q2[$i];
$neg_ew_asy_err[$i] = $err_neg[$i]/$q2[$i];
# $ewinv_pos[$i] = $ewinv_pos[$i]/$q2[$i];
# $ewinv_neg[$i] = $ewinv_neg[$i]/$q2[$i];

printf OUTPOS "%1s %10.6f %10.6f %10.6f\n", $i, $pos_ew_asy[$i], $pos_ew_asy_err[$i],                                  $ewinv_pos[$i];
printf OUTNEG "%1s %10.6f %10.6f %10.6f\n", $i, $neg_ew_asy[$i], $neg_ew_asy_err[$i],                                  $ewinv_neg[$i];
    } #for

    close(INPOS) || die "Can not close INPOS\n";
    close(INNEG) || die "Can not close INNEG\n";
    close(OUTPOS) || die "Can not close OUTPOS\n";
    close(OUTNEG) || die "Can not close OUTNEG\n";

} #foreach
    } #foreach
} #foreach
```

E Code to Add Results for Positive and Negative Target Polarizations

```
#! /usr/local/bin/perl

##############################################################################
# add.pl
# Adds Positive and Negative Electroweak Asymmetries
# Inputs the div* files
# Outputs to add* files
##############################################################################

$c_bin = 0;
$c_ewasy = 1;
$c_err = 2;
$c_ewasyinv = 3;

foreach $energy (29,32){
    foreach $targtype ("li","nh"){
foreach $spect (1,2,3){

    open( INPOS, "div_pos\_$energy\_$targtype\_$spect.out" ) || die "bad input1\n";;
    open( INNEG, "div_neg\_$energy\_$targtype\_$spect.out" ) || die "bad input2\n";
    open( OUT, ">add\_$energy\_$targtype\_$spect.out" )         || die "bad output1\n";

    while(<INPOS>){
@line = split(/\s+/,$_);
$bin = $line[$c_bin];
$ewasy_pos[$bin] = $line[$c_ewasy];
$err_pos[$bin] = $line[$c_err];
$ewasyinv_pos[$bin] = $line[$c_ewasyinv];
    } #while

     while(<INNEG>){
@line = split(/\s+/,$_);
$bin = $line[$c_bin];
$ewasy_neg[$bin] = $line[$c_ewasy];
$err_neg[$bin] = $line[$c_err];
$ewasyinv_neg[$bin] = $line[$c_ewasyinv];
    } #while

    for($i=1;$i<39;$i++){
if($err_pos[$i] == 0){next};
if($err_neg[$i] == 0){next};
if($ewasyinv_pos[$i] == 0){next};
if($ewasyinv_neg[$i] == 0){next};

$factor = 1;
if($energy == 29 ) { $factor=-1;}
# if($spect == 1 || $spect == 3) {$factor = -1;}}
# if($energy == 32 ) {
# if($spect == 2) {$factor = -1;}
# $avg[$i] = ($ewasy_pos[$i] + $ewasy_neg[$i])/(abs($ewasyinv_pos[$i]) + abs($ewasyinv_neg[$i]));
$avg[$i] = ($ewasy_pos[$i] - $ewasy_neg[$i])/($ewasyinv_pos[$i] - $ewasyinv_neg[$i]);
$avg[$i] *= $factor;
# $err[$i] = sqrt(($err_pos[$i]**2 + $err_neg[$i]**2))/(abs($ewasyinv_pos[$i] - $ewasyinv_neg[$i]));
$err[$i] = sqrt(($err_pos[$i]**2 + $err_neg[$i]**2))/($ewasyinv_pos[$i] - $ewasyinv_neg[$i]);
```

```
# printf STDOUT "%1i %2s %2i %10.7f %10.7f %1i\n", $energy, $targtype, $spect,                                          $err_pos[$i], $err_neg[$i], $i;

printf OUT "%1s %8.5f %8.5f\n", $i, $avg[$i], $err[$i];
    } #for

} #foreach spect
    } #foreach target type
} #foreach energy
```

F Code to Combine Results from Li and NH Targets

```
#! /usr/local/bin/perl

##############################################################################
# binadd.pl
# Adds the files bins_li.out bins_nh.out together
# Outputs to bins.out
##############################################################################

$c_bin = 0;
$c_x = 1;
$c_ewasy = 2;
$c_err = 3;

#foreach $targtype ("li","nh"){
open( INLI, "bins_li.out" ) || die "bad input1\n";
open( INNH, "bins_nh.out" ) || die "bad input2\n";
open( OUTFILE, ">bin.out") || die "bad output\n";

while( <INLI> ){
    @line = split(/\s+/,$_);
    $bin = $line[$c_bins];
    $x_li[$bin] = $line[$c_x];
    $ewasy_li[$bin] = $line[$c_ewasy];
    $err_li[$bin] = $line[$c_err];
    print "$bin $x_li[$bin] $ewasy_li[$bin] $err_li[$bin]\n";
} #while

while( <INNH> ){
    @line = split(/\s+/,$_);
    $bin = $line[$c_bins];
    $x_nh[$bin] = $line[$c_x];
    $ewasy_nh[$bin] = $line[$c_ewasy];
    $err_nh[$bin] = $line[$c_err];
    print "$bin $x_nh[$bin] $ewasy_nh[$bin] $err_nh[$bin]\n";
} #while

for($i=1;$i<=4;$i++){
    $avg_ewasy_num[$i] = $ewasy_nh[$i]*(1/$err_nh[$i])**2 + $ewasy_li[$i]*(1/$err_li[$i])**2;
    $avg_x_num[$i] = $x_nh[$i]*(1/$err_nh[$i])**2 + $x_li[$i]*(1/$err_li[$i])**2;
    $avg_ewasy_dem[$i] = (1/$err_nh[$i])**2 + (1/$err_li[$i])**2;
    $ewasy[$i] = $avg_ewasy_num[$i]/$avg_ewasy_dem[$i];
    $x[$i] = $avg_x_num[$i]/$avg_ewasy_dem[$i];
    $err[$i] = 1/($avg_ewasy_dem[$i])**(1/2);

    printf OUTFILE "%1s %10.7f %10.7f %10.7f\n", $i, $x[$i], $ewasy[$i], $err[$i];
} #for
```

G Code to Give a Single Final Result

```
#! /usr/local/bin/perl

##########################################################################
# onebin.pl
# Gives one final number for the EW asymmetery
# Reads in from bins.out
##########################################################################

$c_bin = 0;
$c_x = 1;
$c_ewasy = 2;
$c_err = 3;

open(INFILE, "bin.out") || die "Could not open bins.out\n";

while( <INFILE> ){
    @line = split(/\s+/,$_);
    $bin = $line[$c_bins];
    $x[$bin] = $line[$c_x];
    $ewasy[$bin] = $line[$c_ewasy];
    $err[$bin] = $line[$c_err];
} #while

for($i=1;$i<=4;$i++){
    $ewasy_num += $ewasy[$i]*(1/$err[$i])**2;
    $ewasy_dem += (1/$err[$i])**2;
    $x_num += $x[$i]*(1/$err[$i])**2;
} #for

$x = $x_num/$ewasy_dem;
$ewasy = $ewasy_num/$ewasy_dem;
$err = 1/($ewasy_dem)**(1/2);

printf STDOUT "%10.7f %10.7f %10.7f\n", $x, $ewasy, $err;
```

References

[1] J. Ashman *et al.* [European Muon Collaboration], "An investigation of the spin structure of the proton in deep inelastic scattering of polarized muons on polarized protons," Nucl. Phys. **B328**, 1 (1989).

[2] B. Adeva *et al.* [Spin Muon Collaboration], "A next-to-leading order QCD analysis of the spin structure function g_1," Phys. Rev. **D58**, 112002 (1998).

[3] P. L. Anthony *et al.* [E142 Collaboration], "Deep inelastic scattering of polarized electrons by polarized ^{3}He and the study of the neutron spin structure," Phys. Rev. **D54**, 6620 (1996)

[4] K. Abe *et al.* [E143 collaboration], "Measurements of the proton and deuteron spin structure functions g_1 and g_2," Phys. Rev. **D58**, 112003 (1998) [hep-ph/9802357].

[5] K. Abe *et al.* [E154 Collaboration], "Next-to-leading order QCD analysis of polarized deep inelastic scattering data," Phys. Lett. **B405**, 180 (1997) [hep-ph/9705344].

[6] P. L. Anthony *et al.* [E155 Collaboration], "Measurement of the deuteron spin structure function $g_1^d(x)$ for $1-(GeV/c)^2 < Q^2 < 40-(GeV/c)^2$," Phys. Lett. **B463**, 339 (1999) [hep-ex/9904002].

[7] K. Ackerstaff *et al.* [HERMES Collaboration], "Measurement of the neutron spin structure function g_1^n with a polarized ^{3}He internal target," Phys. Lett. **B404**, 383 (1997) [hep-ex/9703005].

[8] A. Airapetian *et al.* [HERMES Collaboration], "Measurement of the proton spin structure function g_1^p with a pure hydrogen target," Phys. Lett. **B442**, 484 (1998) [hep-ex/9807015].

[9] R. Arnold, *et al.* "A Proposal for Extension of E155 to Measure the Transverse Spin Structure Functions of the Proton and Deuteron," (1997).

[10] B. Adeva *et al.* [Spin Muon Collaboration], 'Spin asymmetries A_1 of the proton and the deuteron in the low x and low Q^2 region from polarized high energy muon scattering," Phys. Rev. **D60**, 072004 (1999).

[11] M. J. Alguard *et al.*, "Elastic scattering of polarized electrons by polarized protons," Phys. Rev. Lett. **37**, 1258 (1976).

[12] G. Baum *et al.*, "A new measurement of deep inelastic e p asymmetries," Phys. Rev. Lett. **51**, 1135 (1983).

[13] R. Arnold, *et al.*, "DIS-Parity: Parity Violation in deep inelastic electron scattering," SLAC-PROPOSAL-E-149 (1993).

[14] L. Sorrell, "Spin Structure Measurements from E155 at SLAC," Conference Proceedings ICHEP (1998).

[15] S. Rock, "The Spin Structure Function g_2 From SLAC E155X" Moriond Conference, March 18-25, 2000, in Les Arcs, Savoie,France

[16] S. Wandzura and F. Wilczek, "Sum Rules For Spin Dependent Electroproduction: Test Of Relativistic Constituent Quarks," Phys. Lett. **B72**, 195 (1977).

[17] H. L. Lai *et al.* [CTEQ Collaboration], "Global QCD analysis of parton structure of the nucleon: CTEQ5 parton distributions," Eur. Phys. J. **C12**, 375 (2000) [hep-ph/9903282].

[18] R. N. Cahn and F. J. Gilman, "Polarized Electron - Nucleon Scattering In Gauge Theories Of Weak And Electromagnetic Interactions," Phys. Rev. **D17**, 1313 (1978).

[19] Private communication with Peter Bosted (Spring 2000).